ELSEVIER

Applied Surface Science 166 (2000) 354–362

applied surface science

www.elsevier.nl/locate/apsusc

Organic semiconductor interfaces: electronic structure and transport properties

I.G. Hill [a,*], D. Milliron [b], J. Schwartz [b], A. Kahn [a]

[a] *Department of Electrical Engineering, Princeton University, Engineering Quadrangle, Olden Street, Princeton, NJ 08544, USA*
[b] *Department of Chemistry, Princeton University Princeton, NJ 08544, USA*

Abstract

Ultraviolet photoelectron spectroscopy (UPS) and X-ray photoelectron spectroscopy (XPS) have been used to investigate a wide range of metal/organic and organic/organic semiconductor interfaces. UPS was used to determine the binding energies of the highest occupied molecular orbitals and vacuum level positions, while XPS was used to find evidence of chemical interactions at these heterointerfaces. It was found that, with a few exceptions, the vacuum levels align at most organic/organic interfaces, while strong interface dipoles, which abruptly offset the vacuum level, exist at virtually all metal/organic semiconductor interfaces. Furthermore, strong dipoles exist at metal/organic semiconductor interfaces at which the Fermi level is completely unpinned within the semiconductor gap implying that the dipoles are not the result of populating or emptying Fermi level-pinning gap states.

Keywords: Organic semiconductor interfaces; UPS; XPS; Transport

1. Introduction

Molecular organic semiconductors have become a very active area of research during the past decade. The recent interest in these materials originates from their potential for use in organic light-emitting devices (OLEDs), in particular for flat-panel display application [1]. In response to the technological success of these materials, fundamental research, with the goal of understanding the surface and interface properties of these systems, has followed. Such studies have proven to be valuable to the device engineers, as well as fundamentally interesting to the semiconductor physicist.

Surface science investigations of organic semiconductor interfaces were initially approached and interpreted in the context of accepted models of inorganic semiconductor interfaces. In particular, metal/organic semiconductor interfaces were studied for a given organic semiconductor and a series of metals, which span a wide range of work functions, to determine whether or not the Fermi level was pinned within the semiconductor gap, and whether or not the vacuum levels of the organic and metal align [2,3]. Prior to these direct measurements, device engineers implicitly assumed that the vacuum levels aligned at metal/organic interfaces, and that ideal Schottky–Mott behavior would result. Similarly, vacuum level alignment was assumed at all organic/organic heterointerfaces.

In this paper, we will describe our studies of organic semiconductor interfaces and summarize our

* Corresponding author. Tel.: +1-609-258-2152; fax: +1-609-258-6279.
E-mail address: ianhill@ee.princeton.edu (I.G. Hill).

0169-4332/00/$ - see front matter
PII: S0169-4332(00)00449-9

findings. Our current understanding of the mechanisms that control molecular level alignment at these interfaces will be described. In addition, we will discuss our efforts to analyze processes that are known to alter the alignment of these levels, with the goal of controlling charge injection characteristics of metal/organic contacts.

2. Experiment

All sample preparation and analysis were performed in an interconnected system of three ultrahigh vacuum chambers. Metal and organic layers were deposited in either the growth or preparation/introduction chambers (base pressures mid 10^{-10} Torr), and all spectroscopies were performed in the main analysis chamber (base pressure 4×10^{-11} Torr), equipped with a He discharge lamp (21.22 eV; 40.8 eV), an X-ray source (Al Kα, 1486.6 eV; Zr Mζ, 151.4 eV), and a double-pass cylindrical mirror analyzer, used for both ultraviolet photoelectron spectroscopy (UPS) and X-ray photoelectron spectroscopy (XPS) studies. The overall resolution was ≈ 150 meV for UPS and ≈ 0.7 eV for XPS. All materials were evaporated or sublimed from thermal deposition sources. The thickness of each film was determined by timed deposition calibrated using a quartz crystal microbalance. No correction for sticking coefficients differing from unity was applied.

In the set of experiments concerning organic-on-metal interfaces, the initial substrates were Si(100) wafers on which 300 Å Cr followed by 1000 Å Au were deposited, giving flat and clean conducting starting surfaces with good optical quality. Experiments on ITO modification were performed on commercial ITO (1500 Å)/glass substrates (Applied Films; 20 $\Omega/\square$).

A typical study of an interface formed by the deposition of an organic semiconductor on a metal surface was performed as follows. A 300-Å thick layer of the metal to be studied was deposited on the Si:Cr:Au substrate. The quality and work function of the base layer were determined using UPS and XPS. A thin layer of organic (typically 2–4 Å) was then deposited on the clean metal substrate, and the spectroscopies repeated. The deposition of organic continued, doubling the total organic thickness at each step, and photoelectron spectra were collected at each thickness. This procedure was repeated until the spectra were characteristic of the organic overlayer, and no contribution from the metal base layer was observed. The data were then compiled and the position of the organic highest occupied molecular orbital (HOMO) and vacuum level relative to the metal Fermi level were determined at each film thickness. In these experiments, the HOMO position is conventionally (and admittedly arbitrarily) taken as the intercept between the tangent to the leading edge of the lowest binding energy feature of the spectrum and the zero-intensity background line. This lowest binding energy feature results from the contribution of one molecular level (i.e., the HOMO), or several closely spaced levels, broadened by thermal effects, random disorder, surface vs. bulk shift, and experimental broadening. The results of these or-

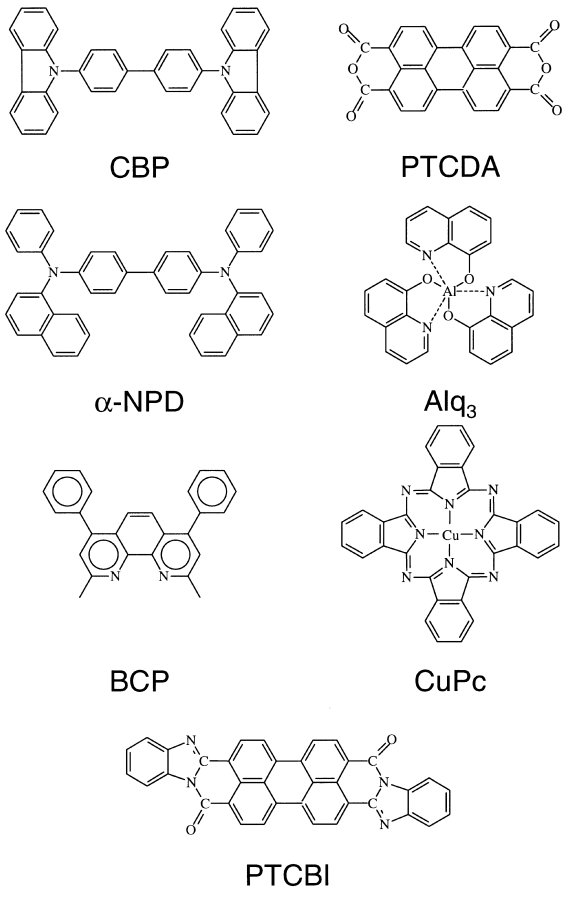

Fig. 1. Molecular structures of the organic semiconductors referred to in this paper.

ganic-on-metal experiments were then interpreted in terms of interface dipoles, for abrupt changes in the vacuum level at the interface, and band bending (in analogy with inorganic semiconductors). If band bending was present, its contribution was subtracted and the position of the organic HOMO at the interface was determined. Studies of organic/organic heterointerfaces were performed using the same procedure, with the base metal layer being replaced with a 100 Å thick organic layer. This layer was thinner than the metal layer used in metal/organic studies to reduce the possibility of charging in the organic layers. The molecular structures of the organic materials used in these experiments are presented in Fig. 1.

3. Results and discussion

3.1. Metal / Organic Semiconductor Interfaces

In this paper, we restrict our discussion of metal/organic interfaces to those formed by depositing organic materials on metals. The interpretation of interfaces formed by the opposite deposition sequence is often complicated by interdiffusion of metal atoms into the organic material. Such interfaces have been described elsewhere [4,5].

The UPS spectra collected during a typical experiment, the interface formed by depositing 4,4′-*N*,*N*′-dicarbazolyl-biphenyl (CBP) on Au, are presented in Fig. 2. The UPS spectrum of the clean Au surface is shown at the bottom of the figure. The Fermi level is clearly visible, and the work function of the surface was determined to be 4.9 ± 0.1 eV. The deposition of 4 Å of CBP on this surface significantly alters the spectrum. The valence region now consists of the superposition of CBP and Au derived features. More significantly, however, the onset of photoemission (low kinetic energy cut-off) shifts abruptly to lower energy by 0.5 eV. This indicates an abrupt shift in the vacuum level, which occurs within the first molecular layer at the interface. Such shifts are interpreted as interface dipoles. As the organic layer thickness increases, the molecular levels, including the HOMO become identifiable. However, it is clear that in some instances, as for example in the case

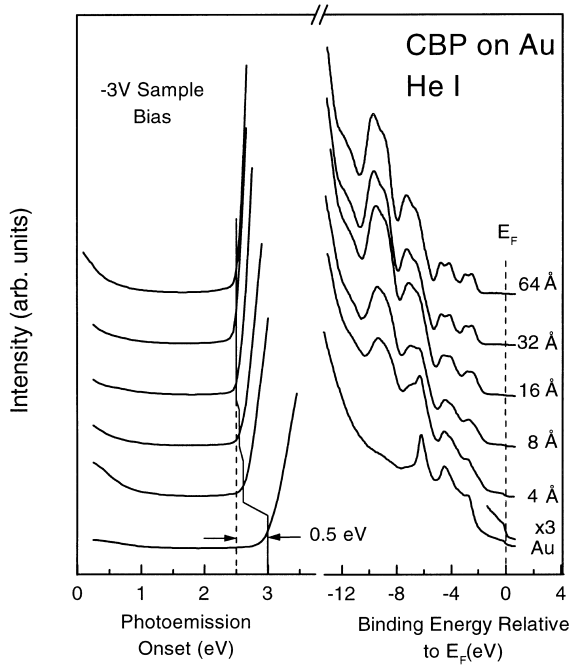

Fig. 2. He I (21.22 eV) UPS spectra for the deposition of CBP on Au. The interface dipole (0.5 eV) is indicated.

presented in Fig. 2, the direct measurement of the HOMO-to-Fermi level barrier at the interface is made difficult by the superposition of the HOMO on the large density of state of the metal. A similar problem occurs at organic/organic interfaces when the HOMOs of the two materials overlap. The method, in these cases, consists of recording the position of one or several deeper features, such as the 9.5 eV molecular peak of CBP (Fig. 2), with respect to the Fermi level (or to the substrate HOMO in the case of an all organic interface). The energy difference between such a peak and the frontier orbital is a fixed characteristic of the material and thus can be used for an accurate measure of the interface position of the HOMO. It should also be noted that charge transfer or chemical interaction could significantly alter the frontier valence levels of the molecules in contact with the metal surface. In these cases, the HOMO may not be identifiable in the first layer. Finally, the observation of several molecular features, such as the one mentioned above, also allows an accurate assessment of band bending in the overlayer away from the interface.

In Fig. 3, we present a summary of the molecular level alignment between four organics (3,4,9, 10-perylenetetracarboxy dianhydride [PTCDA], tris(8-hydroxy-quinoline)aluminum [Alq_3], N,N'-diphenyl-N,N'-bis(l-naphthyl)-l,l′biphenyl-4,4″diamine [α-NPD], and CBP) and metals with work functions ranging from ≈ 3.7 to 5.2 eV. The data are presented as follows. For each organic, the top of the HOMO is plotted at the zero of the vertical energy scale. The lowest unoccupied molecular orbital (LUMO) energy is plotted, assuming a HOMO–LUMO separation equal to the photon energy at the onset of optical absorption. The area between the two levels then represents the organic semiconductor band gap. The measured position of the Fermi level within the gap for metals of different work functions (horizontal axis) are plotted, as well as the expected position predicted in the Schottky–Mott limit (vacuum level alignment; dashed lines). The vertical lines drawn from each experimental data point represent the magnitude of the measured interface dipole. In principal, the magnitude of the interface dipole should be equal to the vertical distance between the experimental Fermi level position and the Schottky–Mott limit.

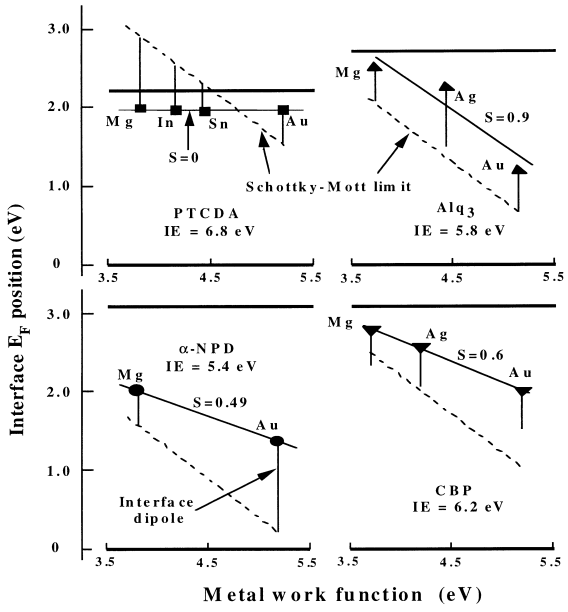

Fig. 3. Measured Fermi level positions at interfaces between various metals and four organic semiconductors.

A best-fit line is also drawn to the experimental points for each organic. The slope of this line (the S parameter is equal to $-1 \times$ slope) is an indication of the ability of the Fermi level to move within the semiconductor band gap. The presence of states within the gap, due to either a large density of bulk impurities, or interfacial gap states, perhaps caused by chemical interactions between the metal and the organic, will tend to reduce the ability of the Fermi level to move. In the limiting case, a very high density of such states will completely pin the Fermi level. As the Fermi level attempts to move, these states will either be populated more or less, depending on the direction of the attempted move. A region of net space charge will occur at the interface, resulting in a localized interface dipole region, which offsets the vacuum levels of the metal and organic, allowing the Fermi levels of the two materials to align without the Fermi level in the organic moving from its pinned position. In the other extreme, a complete absence of gap states will allow the Fermi level to move freely within the gap.

Referring to Fig. 3, we see a wide range of Fermi level behavior. In the case of interfaces between PTCDA and metals ranging from ≈ 3.7 to > 5 eV,

we find that the Fermi level is completely pinned, occurring ≈ 2 eV above the top of the HOMO at all interfaces. The *S* parameter is, therefore, ≈ 0. In contrast, we find that the Fermi level is free to move within the gap of Alq_3, having an *S* parameter of ≈ 0.9. The other two organics represent intermediate cases, with α-NPD having a slope parameter of 0.49, and CBP 0.6. All systems studied contain strong interface dipoles that exceed 1 eV in some cases. It is obvious that the assumption of vacuum level alignment is not a good approximation from which to model OLED behavior.

Returning to the interfaces between Alq_3 and metals, it is interesting to note that these interfaces exhibit large interface dipoles despite the nearly complete freedom with which the Fermi level moves within the gap. It is, therefore, clear that the origin of this dipole is not the emptying or filling of gap states, which, if present in a high enough density to result in such strong dipoles, would also necessarily pin the Fermi level. It is also interesting to note that the magnitude of these dipoles is relatively insensitive to the metal on which the organic is deposited. If the dipole resulted from a chemical interaction with the base metal, one would expect a strong dependence of the magnitude on the reactivity of the metal. To reconcile these observations, it has been suggested that such dipoles are the result of the polarization of the first few molecular layers caused by the electronic image potential at the metallic surface [2].

3.2. Organic / organic Semiconductor Interfaces

UPS spectra collected during a typical investigation of an organic/organic heterointerface (α-NPD on copper phthalocyanine [CuPc]) are presented in Fig. 4. In this case, only the top of the valence structure is shown. One clearly sees the coexistence of the two organic HOMOs at intermediate coverage, with the intensity of the CuPc HOMO diminishing as the α-NPD HOMO intensity increases at higher coverage. Note that the CuPc base layer is not completely suppressed even at a nominal α-NPD thickness of 48 Å. This may indicate that the sticking coefficient of α-NPD on CuPc is significantly less than unity, or that the α-NPD evolves via 3D island growth, such that the CuPc features are not suppressed until the islands coalesce. This distinction does not complicate the analysis here, as there is no band-bending contribution, the analysis of which would require a knowledge of the true thickness. The morphology of the resulting interface may, however, have an impact on devices constructed using such an interface.

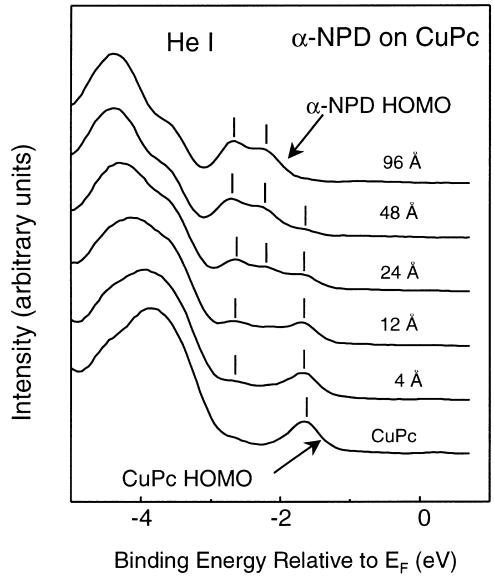

Fig. 4. He I (21.22 eV) UPS spectra showing the evolution of the top of the valence spectra for the interface formed by depositing α-NPD on CuPc.

A summary of the alignment of organic levels at twelve organic/organic heterointerfaces is presented in Fig. 5 [6–9]. We have found that, within our experimental uncertainty of 0.1 eV, the vacuum levels align at almost all organic/organic heterointerfaces. This is not too surprising, considering the closed-shell nature of the molecules that comprise both constituents of the heterointerface. Charge exchange and/or chemical bonding between different molecular species is not expected. Perhaps the most interesting cases are those where measurable dipoles do exist: CuPc/PTCDA (0.4 eV), PTCDA/Alq_3 (-0.5 eV), α-NPD/Alq_3 (-0.25 eV), and BCP/PTCBI (bathocuproine/3,4,9,10 perylenetetracarboxylic bisbenzimidazole) (0.4 eV) where the dipole is defined as positive when the vacuum level of the second material is at a higher energy that the first. Ishii et al. [2] recognized that dipoles often occur at

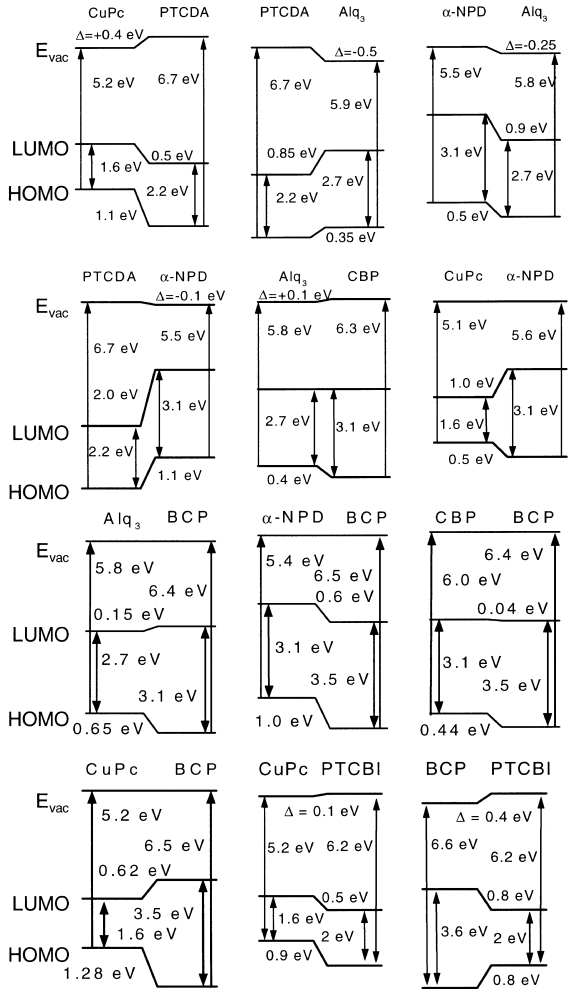

Fig. 5. The alignment of molecular levels at 12 organic/organic heterointerfaces.

heterointerfaces between two materials of greatly differing ionization energies and electron affinities, which are referred to as donor/acceptor interfaces. At such interfaces, an electron may be expected to be (partially) transferred from the low ionization energy constituent to the high electron affinity molecule. Indeed, this argument may be used to explain the dipoles which we have measured between the high electron affinity molecule, PTCDA, and the lower ionization energy molecules, CuPc and Alq_3. However, if we believe this mechanism to be responsible for the observed dipoles, we would then predict that the PTCDA/α-NPD interface should also contain a strong dipole, given that α-NPD has a lower ionization energy and electron affinity compared to Alq_3. This prediction contradicts our observation of a negligible dipole at this interface. We have noted that three of the constituents of the interfaces possessing dipoles also exhibit a limited range of Fermi level movement at heterointerfaces (PTCDA, PTCBI, BCP). It is therefore possible that the Fermi levels of these materials are pinned by impurity related gap states, and the dipoles are the result of (de)populating a high density of impurity states near the interfaces. The 0.5-eV dipole observed at the PTCDA/Alq_3 interface cannot be explained on this basis, given the above observation that the Fermi level is completely free to move within the Alq_3 gap. Considering the mechanisms suggested above, and the counter examples, one must conclude that neither of the suggested mechanisms for dipole formation at organic/organic heterointerfaces is sufficient to explain all of the observed behavior.

3.3. Modifying Interfaces

One of the areas where surface scientists may have the greatest impact on the technology of organic light emissive materials is in interface engineering. The goal of this research is to control the injection and transport properties at metal/organic and organic/organic semiconductor interfaces, respectively. The approaches used to date include chemically altering the surface of an injecting contact, such as oxygen plasma treatment of indium tin oxide (ITO) [10–13], inserting thin organic layers between an injecting contact and the main organic layer [9,14,15], and including sub-monolayer quantities of alkali halides or alkali metals at an interface [16–19]. All of these techniques were originally introduced by the device engineers, and later explained by the surface scientists. In the future, perhaps the roles will reverse, with the surface scientist providing the insight to improve the engineers' devices. The following will describe our combined use of several surface science techniques, along with simple electrical transport measurements, to build a coherent understanding of one such system.

We have recently completed a study of the effects of oxygen plasma treatment on the surface of ITO. A consensus that the process increased the work function of the pseudo-metal surface by ≈ 0.5 eV, in agreement with its improved hole injection contact properties [10,20] had been reached, but the source of this change was still a matter of some debate. Proposed explanations included the presence or absence of hydroxyl groups on the surface [21] and changes in surface stoichiometry [11,12].

In contrast to these proposals, our XPS studies did not identify any systematic change in surface stoichiometry with oxygen plasma treatment of the ITO surface, although variations from sample to sample of this ill-defined, non-stoichiometric ternary oxide were observed. In addition, we were able to controllably remove (dehydroxylate) and reintroduce (rehydroxylate) the surface hydroxyl groups in UHV. The hydroxyl groups were easily removed by mild Ar ion sputtering (0.5 kV, 1 $\mu A/cm^2$, 15 min). The absence of surface hydroxyl groups after sputtering was confirmed by the change in the composition of the O (1s) core level XPS spectrum, and by FTIR analysis, which indicated the loss of an O–H stretching mode feature at 3379 cm^{-1}. Rehydroxylation was accomplished by dosing the freshly sputtered ITO surface at low temperature, in UHV, with water and subsequently warming the sample to desorb the excess water. Again, rehydroxilation was confirmed by XPS and FTIR analysis.

The results of our studies of the as-received, oxygen plasma treated, dehydroxylated and rehydroxylated ITO surfaces are summarized in Fig. 6. We confirm the earlier finding that the ITO work function is increased by 0.5 eV following oxygen plasma treatment. However, we have found that the as-received, dehydroxylated, and rehydroxylated surfaces have, within our experimental uncertainty of 0.1 eV, identical work functions. The presence of hydroxyl groups on the surface of the ITO therefore does not significantly affect its work function. Additionally, by studying the initial stages of growth of α-NPD on each surface, we have found that the hole

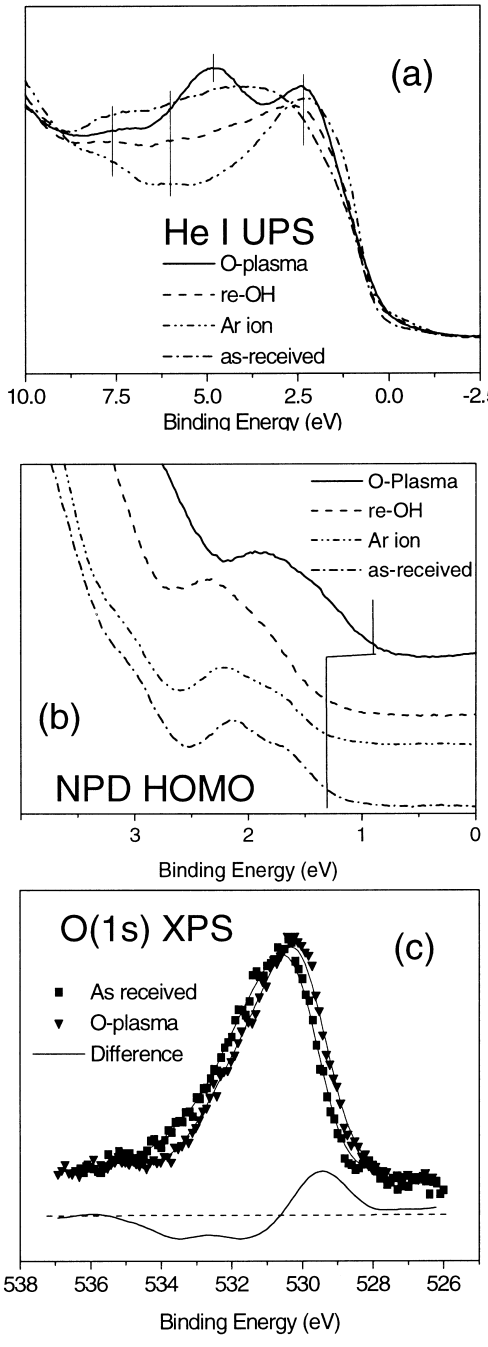

Fig. 6. Summary of a surface studies of as-received, Ar ion sputtered, rehydroxylated, and oxygen plasma treated ITO. (a) The He I UPS data of the clean surfaces are presented with the binding energy (BE) referenced to the top of the valence band. (b) The He I UPS data showing the α-NPD HOMO level are plotted with the binding energies relative to the Fermi level. (c) The O (1s) core levels of the as-received and oxygen plasma treated surfaces are presented, along with their difference.

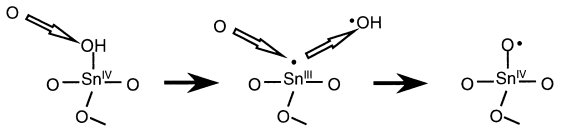

Fig. 7. Oxygen plasma treatment of ITO. The OH groups are first sputtered by the high energy O atoms. The resulting Sn^{III} sites immediately react with O atoms from the plasma, forming the Sn^{IV}–O· species, which increase the surface work function.

injection barrier from the oxygen plasma treated surface is 0.5 eV smaller than those on the other three surfaces (Fig. 6b), in agreement with the observed change in work function. Current–voltage (I–V) measurements of simple hole-only devices built on each surface confirm the superior injection properties of the oxygen plasma treated surface.

Closer examination of the O (1s) and Sn (3d) core levels of the four surfaces provided insight into the plasma treating process. Slight differences between the Sn (3d) core levels on dehydroxylated and rehydroxylated surfaces were observed, although no change in the In (3d) core level was noted, suggesting that the hydroxyl groups are bound to surface Sn atoms. Further evidence was found by an independent measurement of the surface hydroxyl concentration [13], which agreed, within error, with the expected surface Sn atom concentration (note that In:Sn ≈ 10). The high binding energy side of the O (1s) peak (Fig. 6c), corresponding to the surface hydroxyl content, differed from surface to surface, with the as-received and rehydroxylated surfaces having a much higher hydroxyl contribution than the oxygen plasma treated and dehydroxylated surfaces. The low binding energy side of the peak, however, was identical on all surfaces except those having undergone oxygen plasma treatment. On the plasma treated surfaces, the low binding energy side of the peak increased in intensity (Fig. 6c), which we attribute to a new, lower binding energy, O radical (O·) species on the surface which replaces the hydroxyl groups during the oxygen plasma treatment. This proposal is supported by a new UPS valence feature present on the oxygen plasma treated surfaces at ≈ 4.8 eV below the top of the valence band (Fig. 6a), in a region of the valence band which has previously been assigned to O (2p) derived states in pure In_2O_3 [22]. The proposed chemical explanation of the oxygen plasma process is outlined in Fig. 7. Preliminary calculations of the dipole moment associated with this stable surface radical system indicate that the surface density required to increase the work function by 0.5 eV is in excellent agreement with the surface density of Sn atoms, and therefore the original hydroxyl density.

4. Conclusion

Traditional surface science techniques have been successfully used to study the surfaces and interfaces of organic semiconductors. Systematic studies of the interfaces between metals and organic semiconductors have revealed that large interface dipoles are present at virtually all interfaces. In contrast, the vacuum levels are found to align at most organic/organic heterointerfaces. The source of the interface dipoles observed at a few of these interfaces is not understood. Combined UPS/XPS and transport studies of the oxygen plasma treated ITO surface have revealed that the work function is increased by a change in surface chemistry, which results in a stable oxygen radical species bound to Sn surface sites.

Acknowledgements

Support of this work by the MRSEC program of the National Science Foundation (award #DMR-9809483) and by the New Jersey Center for Optoelectronics (grant #97-2890-051-17) is gratefully acknowledged. One of the authors (I.H.) acknowledges support from NSERC of Canada. The authors also thank the groups of S.R. Forrest and M.T. Thompson for providing the organic materials.

References

[1] R. Forrest, Chem. Rev. 97 (1997) 1793.
[2] H. Ishii, K. Sugiyama, D. Yoshimura, E. Ito, Y. Ouchi, K. Seki, IEEE J. Sel. Top. Quantum Electron. 4 (1998) 24.
[3] I.G. Hill, A. Rajagopal, Y. Hu, A. Kahn, Appl. Phys. Lett. 73 (1998) 662.
[4] A. Rajagopal, A. Kahn, J. Appl. Phys 84 (1998) 355.

[5] Y. Hirose, A. Kahn, V. Aristov, P. Soukiassian, V. Bulovic, S.R. Forrest, Phys. Rev. B 54 (1996) 13748.
[6] A. Rajagopal, C.I. Wu, A. Kahn, J. Appl. Phys 83 (1998) 2649.
[7] A. Rajagopal, A. Kahn, Adv. Mater. 10 (1998) 140.
[8] I.G. Hill, A. Kahn, J. Appl. Phys 84 (1998) 5583.
[9] I.G. Hill, A. Kahn, J. Appl. Phys. 86 (1999) 2116.
[10] J.S. Kim, M. Granström, R.H. Friend, N. Johansson, W.R. Salaneck, R. Daik, W.J. Feast, F. Cacialli, J. Appl. Phys. 84 (1998) 6859.
[11] C.C. Wu, C.I. Wu, J.C. Sturm, A. Kahn, Appl. Phys. Lett. 70 (1997) 1348.
[12] F. Steuber, J. Staudigel, M. Stössel, J. Simmerer, A. Winnacker, Appl. Phys. Lett. 74 (1999) 3558.
[13] D. Markiewicz, I.G. Hill, A. Kahn, J. Schwartz, J. Appl. Phys. 87 (2000) 572.
[14] I.H. Campbell, J.D. Kress, R.L. Martin, D.L. Smith, N.N. Barashko, J.P. Ferraris, Appl. Phys. Lett. 71 (1997) 3528.
[15] L.S. Hung, C.W. Tang, M.G. Mason, Appl. Phys. Lett. 70 (1997) 152.
[16] I. Haskal, A. Curioni, P.F. Seidler, W. Andreoni, Appl. Phys. Lett. 71 (1997) 1151.
[17] G.E. Jabbour, Y. Kawabe, S.E. Shaheen, J.F. Wang, M.M. Morrell, B. Kippelen, N. Peyghambarian, Appl. Phys. Lett. 71 (1997) 1762.
[18] L.S. Hung, C.W. Tang, M.G. Mason, Appl. Phys. Lett. 70 (1997) 152.
[19] T. Mori, H. Fujikawa, S. Tokito, Y. Taga, Appl. Phys. Lett. 73 (1998) 2763.
[20] M. Stössel, J. Staudigel, F. Steuber, J. Simmerer, G. Wittmann, A. Kanitz, H. Klausmann, W. Rogler, W. Roth, J. Schumann, A. Winnacker, PCCP 1 (1999) 1791.
[21] F. Nüesch, L.J. Rothberg, E.W. Forsythe, Q.T. Le, Y. Gao, Appl. Phys. Lett. 74 (1997) 880.
[22] H. Öfner, J. Kraft, R. Hofmann, S.L. Surnev, F.P. Netzer, J.J. Paggel, K. Horn, Surf. Sci. 316 (1994) 112.